Efficient Inverse Analysis for Solving a Coupled Conduction, Convection and Radiation Problem Involving Non-gray Participating Media

HE Zheng[1], *CAO Zhenkun*[1], *CHENG Xiang*[2], *CUI Miao*[1*], *LIU Kun*[1]

1. School of Mechanics and Aerospace Engineering, State Key Laboratory of Structural Analysis, Optimization and CAE Software for Industrial Equipment, Dalian University of Technology, Dalian 116024, P.R. China;
2. Science and Technology on Space Physics Laboratory, CALT, Beijing 100076, P.R. China

(Received 11 May 2024; revised 12 September 2024; accepted 10 October 2024)

Abstract: The presence of non-gray radiative properties in a reheating furnace's medium that absorbs, emits, and involves non-gray creates more complex radiative heat transfer problems. Furthermore, it adds difficulty to solving the coupled conduction, convection, and radiation problem, leading to suboptimal efficiency that fails to meet real-time control demands. To overcome this difficulty, comparable gray radiative properties of non-gray media are proposed and estimated by solving an inverse problem. However, the required iteration numbers by using a least-squares method are too many and resulted in a very low inverse efficiency. It is necessary to present an efficient method for the equivalence. The Levenberg-Marquardt algorithm is utilized to solve the inverse problem of coupled heat transfer, and the gray-equivalent radiative characteristics are successfully recovered. It is our intention that the issue of low inverse efficiency, which has been observed when the least-squares method is employed, will be resolved. To enhance the performance of the Levenberg-Marquardt algorithm, a modification is implemented for determining the damping factor. Detailed investigations are also conducted to evaluate its accuracy, stability of convergence, efficiency, and robustness of the algorithm. Subsequently, a comparison is made between the results achieved using each method.

Key words: inverse problem; coupled heat transfer problem; Levenberg-Marquardt algorithm

CLC number: TK124 **Document code:** A **Article ID:** 1005-1120(2024)05-0621-11

0 Introduction

In certain high temperature surroundings, such as heaters or combustors, it is challenging to accurately ascertain the temperature distribution due to the coupled heat exchange model[1-2]. The case would be deteriorated if absorbing, emitting and non-gray participating media are involved[3-5]. Accurate evaluation of radiative properties of these media[6-7] significantly increases the difficulty in solving the radiative heat transfer problem, as well as the coupled conduction, convection and radiation problem. In addition, the complete simulation could not satisfy the real-time control requirements of reheating furnaces, despite its potential for high accuracy[8-9]. To overcome this difficulty and meet the real-time demand, total heat exchange factor was introduced[10] with the aim of simplifying the complete coupled heat transfer simulation. Besides, an estimation of gray-equivalent radiative properties of non-gray media were made through solving an inverse issue in order to increase the efficiency[11]. However, the number of iterations using a least-squares method was excessive, resulting in a low inverse efficiency[11], which is disadvantageous and restricts the equivalence's engineering applications. If the inverse problem of thermal conductivity, convection and radiation coupling of absorbing, emit-

*Corresponding author, E-mail address: miaocui@dlut.edu.cn.

How to cite this article: HE Zheng, CAO Zhenkun, CHENG Xiang, et al. Efficient inverse analysis for solving a coupled conduction, convection and radiation problem involving non-gray participating media[J]. Transactions of Nanjing University of Aeronautics and Astronautics, 2024, 41(5): 621-631.

http://dx.doi.org/10.16356/j.1005-1120.2024.05.007

ting and non-gray participating media in a reheating furnace is to be solved, it is necessary to propose an effective method.

Numerical methods have been proposed to address the inverse problems, including those related to heat conduction, convection, radiation, and coupled heat transfer problems[12-15], which have wide engineering backgrounds and have been receiving more and more attentions[16-20]. In essence, there are two major types for inverse approaches: Stochastic methods, as exemplified by the genetic algorithm, and gradient-based methods, represented by the conjugate gradient method. The stochastic have the merit of global convergence. Higher precision and efficiency are the benefits of gradient-based algorithms, which are advantageous in engineering applications, especially for real-time occasions[10]. In the above approach, it is necessary to determinate the sensitivity coefficient precisely. For sensitivity analysis in inverse heat transfer problems[21-25], the complex-variable-differentiation method[26] was introduced by the first author and coworkers, enabling the accurate determination of sensitivity coefficients. Numerical examples verified good performances of a few gradient-based methods.

A novel approach to determine the damping factor in the Levenberg-Marquardt algorithm was recently presented[27]. The proposed method was found to enhance the performance of the Levenberg-Marquardt algorithm, as evidenced by the numerical results. The performance of the Levenberg-Marquardt algorithm can be significantly influenced by the manner in which the damping factor is determined[27]. For example, some methods would lead to a very low efficiency, although the convergence stability may be very good. By using the newly proposed formulation in Ref.[27], our findings indicate that the Levenberg-Marquardt algorithm exhibited superior performance among these approaches when applied to solve an inverse heat conduction problem, which was more efficient and more convergence stable. Inspired by this, the Levenberg-Marquardt algorithm[27] is utilized in the current study to recover the comparable gray radiative properties of non-gray media. The inverse problem of coupling heat conduction, convection, and thermal radiation in a heater is solved to accomplish this. It is anticipated that the problem of low inverse efficiency, as demonstrated by the least-squares method outlined in Ref.[11], will be effectively addressed through the application of the Levenberg-Marquardt algorithm.

1 Coupled Conduction, Convection and Radiation Problem

The coupled heat problem of conduction, convection, and radiation in a high temperature reheating furnace is considered. The reheating furnace is comprised of four distinct zones: The preheating zone, the first heating zone, the second heating zone, and the soaking zone. Its key parameters are presented in Table 1.

Table 1 Key parameters of the reheating furnace

Furnace zone	Length/m	Width/m	Height of upper hearth/m	Fuel consumption/($m^3 \cdot h^{-1}$)	Air-fuel ratio
Preheating zone	24	12.8	0.9	1 130.2	2.53
First heating zone	10	12.8	1.9	5 633.84	2.53
Second heating zone	11	12.8	1.45	9 183.95	2.42
Soaking zone	10	12.8	1.45	4 115.88	2.42

The heated slab, with dimensions of 12 m in length, 1.293 m in width, and 0.23 m in depth, enables the production of 370 t of steel per hour. The calorific value of the fuel is 8 800 kJ/m^3.

A heater is designed to reheat slabs that enter from its one side (preheating zone) and move to the exit (soaking zone). Given the interplay of combustion, fluid flow, and coupled heat transfer phenomena[28], mathematical models in reheating furnaces are highly sophisticated[28-30]. Fuels are assumed to be instantaneously burned completely. The gas flows slowly and the velocity is assumed to be a constant. Considering the elevated temperatures present, thermal radiation becomes the major mode of heat transfer, it is critical to precisely specify the radiative

characteristics of combustion gases. Carbon dioxide and water vapor are the main components of the gas, which absorb and emit infrared radiation at specific wavelengths and they are also known as non-gray participating media because their radiative properties vary with wavelengths[14]. The gases flow, and convective heat transfer is conducted between gases and solid surfaces. Heat conduction is conducted in solids, from surface to inside. The analysis above reveals that the coupled heat transfer problem exhibits a highly nonlinear behavior.

The zonal method by introducing imaginary planes[27] is used for solving the radiative transfer problem, and the radiative properties of non-gray media have been evaluated through using the Edwards exponential broadband model (for a single gas) and the Leckner series (corresponding to mixture)[31].

The high temperature system is divided into model zones. In each nearly cubic model zone, there are six surface zones (three walls, two imaginary planes and one slab) and one gas zone (non-gray gas), as shown in Fig.1. Therefore, there are seven energy balance equations.

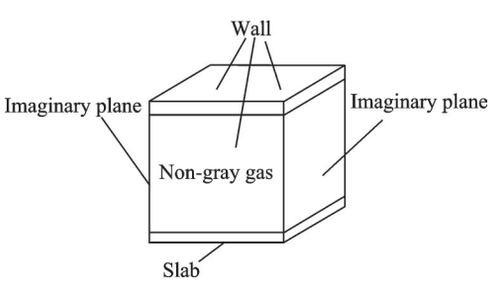

Fig.1 A model zone

The expression of the energy balance equation for the gas region of the ith model region is shown as

$$Q_{r,i}+Q_{com,i}+Q_{a,i}+Q_{f,i}+Q_{mov,i}-Q_{c,i}-Q_{store,i}=0 \tag{1}$$

where $Q_{store,i}$ is the net heat of the gas zone; $Q_{c,i}$ the convective heat transfer; $Q_{mov,i}$ the heat from the adjacent model zone; $Q_{a,i}$ the heat from the air; $Q_{f,i}$ the heat from fuel; $Q_{com,i}$ the heat from combustion, and $Q_{r,i}$ the radiation of the gas zone with all other zones.

The basic geometrical and operational parameters of the reheating furnace are utilized to solve the coupled heat exchange issue in this paper.

In steady state, the heat flux between the inner surface and the outer surface of each wall is equal to the amount by heat conduction between the inner and outer surfaces. The energy balance for each of the three walls is expressed by

$$\left(\overline{G_iS_l}E_{b_{g_i}}+\sum_{j=1}^{N}\overline{S_jS_l}E_{b_{s_j}}-\overline{S_lG_i}E_{b_{s_l}}-\sum_{j=1}^{N}\overline{S_lS_j}E_{b_{s_j}}\right)\Big/A_{s_l}+h_{s_l}(t_{g_i}-t_{s_l})=\frac{t_{s_l}-t_\infty}{\frac{d_{s_l}}{\lambda_{s_l}}+\frac{1}{\alpha_\infty}} \tag{2}$$

where $\overline{G_iS_l}$, $\overline{S_jS_l}$, $\overline{S_lG_i}$ and $\overline{S_lS_j}$ are the total radiative exchange areas, which are calculated by radiative properties; E_b is the blackbody emissive power; A the model area; h the convective heat coefficient; t the temperature in Celsius; d the depth; λ the thermal conductivity; N the number of surfaces within the model; subscripts ∞, s and g represent the surrounding, surface and non-gray medium, respectively.

The net radiative heat flux of the imaginary plane equals zero when it is considered as a blackbody. This property greatly reduces the computational effort by ensuring that the total radiative exchange between adjacent model domains is correctly described. The energy balance for each of the two imaginary planes is defined as

$$\overline{G_iS_l}E_{b_{g_i}}-\overline{S_lG_i}E_{b_{s_l}}+\left(\sum_{j=1}^{N}\overline{S_jS_l}E_{b_{s_j}}-\sum_{j=1}^{N}\overline{S_lS_j}E_{b_{s_j}}\right)_i+\overline{G_{i-1}S_l}E_{b_{g_{i-1}}}-\overline{S_lG_{i-1}}E_{b_{s_l}}+\left(\sum_{j=1}^{N}\overline{S_jS_l}E_{b_{s_j}}-\sum_{j=1}^{N}\overline{S_lS_j}E_{b_{s_j}}\right)_{i-1}=0 \tag{3}$$

For the slab surface zone, its heat flux consists of the radiative and the convective, as shown in Eqs.(4,5). The convection heat transfer coefficient between the surface and the gas in the zones is determined by using the empirical formula[32].

$$q_{r,s_m}=\frac{\overline{G_iS_m}E_{b_{g_i}}+\sum_{j=1}^{N}\overline{S_jS_m}E_{b_{s_j}}-\overline{S_mG_i}E_{b_{s_m}}-\sum_{j=1}^{N}\overline{S_mS_j}E_{b_{s_m}}}{A_{s_m}} \tag{4}$$

$$q_{c,s_m}=h_{s_m}(t_{g_i}-t_{s_m}) \tag{5}$$

Due to the slight temperature variations along the width and length of the slab, its three-dimensional heat transfer equation can be simplified to a one-dimensional transient form along its depth direction, i.e., Eq.(6), and the y-coordinate represents the axis along the depth of the slab.

$$\rho(t_{\mathrm{mp}})c(t_{\mathrm{mp}})\frac{\partial t_{\mathrm{mp}}(y)}{\partial \tau}=\frac{\partial}{\partial y}\left[\lambda(t_{\mathrm{mp}})\frac{\partial t_{\mathrm{mp}}(y)}{\partial y}\right] \quad (6)$$

The temperature function is given as an initial condition

$$t_{\mathrm{mp}}(y,\tau)|_{\tau=0}=t_{\mathrm{mp}}(y) \quad (7)$$

The boundary conditions are of the second type with heat fluxes containing both convection and radiation applied to the upper and the lower surfaces, respectively.

$$\lambda(t_{\mathrm{mp}})\frac{\partial t_{\mathrm{mp}}(y)}{\partial y}|_{y=d_{S_u}}=q_{\mathrm{u}} \quad (8)$$

$$-\lambda(t_{\mathrm{mp}})\frac{\partial t_{\mathrm{mp}}(y)}{\partial y}|_{y=0}=q_{\mathrm{b}} \quad (9)$$

In Eqs.(6—9), c is the mass specific heat; t_{mp} the temperature function; τ the time; subscripts u and b represent upper and bottom. To solve the transient heat conduction equation of the slab, the finite difference method is employed, which has been previously validated.

The computational procedure for solving the coupled heat exchange issue is shown in Fig.2.

The initial estimated temperature vector, abbreviated as $\boldsymbol{t}_0$, is first assigned to each zone of the model. Subsequently, the non-gray radiative properties are computed, followed by the determination of the total radiative exchange areas; the temperatures of the gas, two hypothetical planes, and three walls in each model zone are determined by solving the energy balance Eqs.(1—3); each model zone's heat flux on the slab's surface is calculated; the computed temperature vector $\boldsymbol{t}$ in each model zone is obtained by solving the slab's heat conduction equation. The iterative procedure continues until the difference between the guessed and calculated temperature vectors is within a specified tolerance. If convergence is not achieved, the guessed temperature vector is updated, and the process is repeated from the beginning.

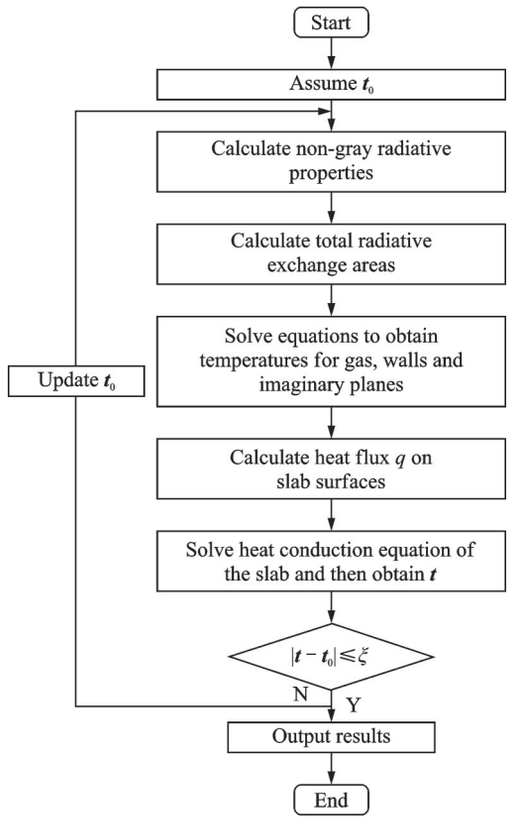

Fig.2 Computational procedure for solving the coupled conduction, convection and radiation problem

The solution methods for solving the coupled conduction, convection and radiation problem were validated in Ref.[11].

2 Levenberg-Marquardt Algorithm

The aim of this research is to propose an effective method to determine the equivalence of non-gray radiative properties. This is achieved by solving an inverse problem that involves the coupling of conduction, convection, and radiation. To solve the inverse issue, the Levenberg-Marquardt algorithm[27] is employed, because it has good performances in solving an inverse heat problem. The temperature simulated by the direct problem solution is taken as the known real temperature in the inverse analysis and the equivalent gray radiation properties of the non-gray media are recovered. The introduction of the minimization problem for the dimensionless objective function in Eq.(10) enables the estimation of comparable gray radiation properties based on simulated temperature measurements.

$$F(x_1,x_2,\cdots,x_K)=$$

$$\sqrt{\frac{1}{M}\sum_{i=1}^{M}\left(\frac{\boldsymbol{t}_i^*-\boldsymbol{t}_i(x_1,x_2,\cdots,x_K)}{\boldsymbol{t}_i^*}\right)^2} \tag{10}$$

where $\boldsymbol{x}=[x_1,x_2,\cdots,x_K]$ is the vector of retrieval parameters; M the overall count of temperature measurements; $\boldsymbol{t}_i$ and $\boldsymbol{t}_i^*$ are the calculated and the simulated measured temperatures, respectively; $i=1,2,\cdots,M$, and K is the total number of parameters to be recovered. The retrieval parameters vector is updated by

$$\{x_k^{P+1}\}=\{x_k^P\}+\{\delta_k^P\} \tag{11}$$

where P represents the iteration number; k ranges from 1 to K, and the value of δ can be obtained by

$$[\boldsymbol{J}^{\mathrm{T}}\boldsymbol{J}+\mu\mathrm{diag}(\boldsymbol{J}^{\mathrm{T}}\boldsymbol{J})]\delta=\boldsymbol{J}^{\mathrm{T}}[\boldsymbol{t}_i^*-\boldsymbol{t}_i(\boldsymbol{x})] \tag{12}$$

where $\boldsymbol{J}$ is sensitivity coefficients matrix. The complex-variable differentiation method is utilized to compute every sensitivity coefficient precisely. The damping factor μ, plays a significant role in the inverse process and may have a significant impact on its performance. Some methods for damping factors may lead to a very low efficiency, thereby reducing the Levenberg-Marquardt algorithm's benefit of generally outstanding precision. Damping factor is determined as

$$\mu=F(\boldsymbol{x})^n \tag{13}$$

The iteration process is halted when either the target function or the difference between F^{P+1} and F^P reaches a given tolerance.

$$F\leqslant\xi \text{ or } |F^{P+1}-F^P|\leqslant\xi \tag{14}$$

Fig.3 illustrates the computational process for handling the inverse issue. The procedure begins with the provision of the initial estimate, x^0, of the equivalent gray emissivities for each model region; next, the direct problem procedure is called and the calculated temperature at the measurement point is obtained; then the objective function F is calculated; when the specified stopping criterion is met, the iterative procedure is terminated; otherwise, calculate $\boldsymbol{J}$ and μ; and obtain δ through solving Eq.(12) afterwards; after that, x^0 is updated, and the process repeats from the beginning.

It is evident that the computational procedure for solving the direct problem is invoked in each inverse analysis.

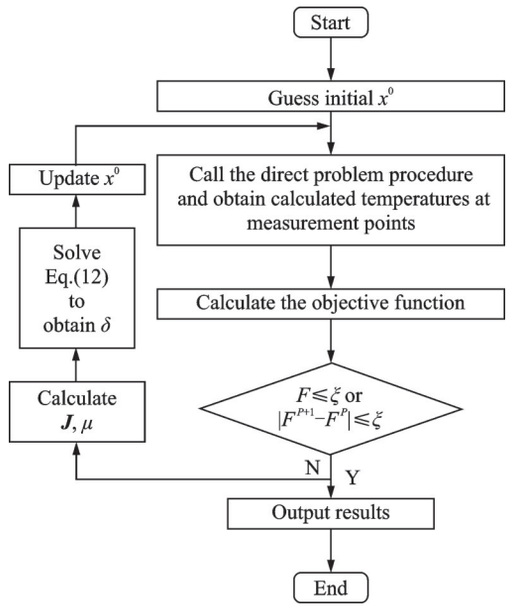

Fig.3 Computational procedure for solving the inverse coupled conduction, convection and radiation problem

3 Results and Discussion

A good inverse approach for a specified problem should be accurate, efficient, convergence stable and robust. Four key aspects of the Levenberg-Marquardt algorithm are explored in this research. Specifically, this study examines the potential of the Levenberg-Marquardt algorithm to address inverse problems associated with coupled conduction, convection, and radiation in the context of absorption, emission, and non-gray participating media.

3.1 Validation of accuracy and efficiency

In this case, the accuracy and efficiency of the algorithm for solving the inverse coupled heat exchange issue is examined. Each model zone is associated with one equivalent gray emissivity. Additionally, there is the total number of 11 equivalent gray emissivity distributed along the furnace's length. In each model zone, there are two measurement points: One locates at the upper surface and the other at the center of the slabs. So the total number of temperature measurements is 22. According to Fig.4, the convergence curves of the 11 parameters are displayed when the Levenberg-Marquardt algorithm is applied. The initial guesses for each parameter are set to 0.2. During the iteration process, the objective function F is decreasing. As shown in Eq.(14), the iteration is stopped until the objective function is

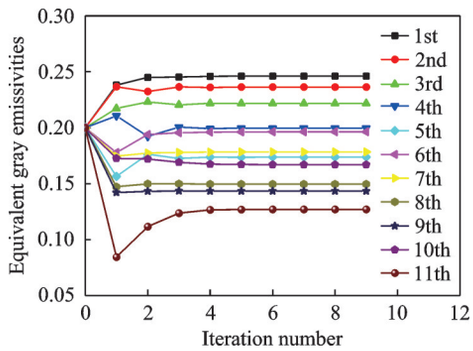

Fig.4 Convergence curves of 11 equivalent gray emissivities with initial guesses as 0.2

within a specified tolerance ξ. The final objective function is 1.297×10^{-5}, which implies the high accuracy of this algorithm.

The measured temperature data are simulated by solving the non-gray gas radiative direct problem, in which a modified zonal method is used to solve the radiative transfer equation (RTE). The calculated temperatures data are those obtained after the iteration of the inverse problem calculations mentioned in Fig.3, using the equivalent gray radiative properties. The calculated and the simulated measured temperatures compete well with each other, as shown in Table 2.

It implies the Levenberg-Marquardt algorithm is highly accurate in terms of equivalent non-gray radiation properties. Furthermore, the algorithm exhibits a remarkable precision when resolving inverse coupled heat exchange issues, which comprise absorption, emission, and non-gray participating medium. This is because the recovered outcomes are equivalent to those achieved by using the least-squares method.

Fig.5 indicates that the total number of iterations of the two algorithms is 9 for one and above 120 for the other when the initial guesses are set to 0.2 for each parameter. It reveals that the Levenberg-Marquardt algorithm is much more efficient than the least-squares method for solving the inverse coupled heat transfer issue. In order to guarantee convergence when solving the inverse problem, the relaxation factor in the least-squares method has to be a very small value. If the relaxation factor becomes smaller, it will result in a low inverse efficiency. Consequently, the efficiency by using the

Table 2 Calculated and simulated measured temperatures

No.	t/℃	
	Simulated measured	Calculated
1	100.32	100.319 5
2	211.13	211.129 2
3	349.01	349.012 4
4	528.99	528.986 6
5	735.66	735.659 4
6	916.09	916.090 0
7	1 041.19	1 041.190 1
8	1 139.27	1 139.271 4
9	1 206.79	1 206.789 6
10	1 231.05	1 231.047 7
11	1 250.93	1 250.930 1
12	44.36	44.358 0
13	129.65	129.654 2
14	235.27	235.265 1
15	365.15	365.151 2
16	519.32	519.323 3
17	681.32	681.320 2
18	829.52	829.520 7
19	966.77	966.770 0
20	1 087.60	1 087.595 6
21	1 168.79	1 168.793 7
22	1 212.90	1 212.901 0

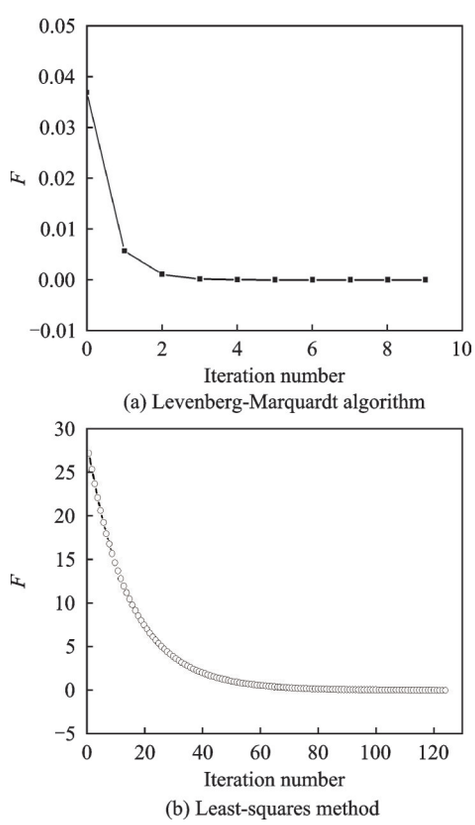

Fig.5 Objective function with the iteration number

least-squares method is much lower. On the other hand, the formulation described in Ref.[27] for determining the damping factor in the Levenberg-Marquardt algorithm could guarantee both high efficiency and good convergence stability.

3.2 Validation of convergence stability

In this section, we examine the impact of the initial guess on the inverse results to assess the convergence stability of the Levenberg-Marquardt algorithm for the equivalence of non-gray radiative properties. Other initial guesses are examined, 0.000 01, 0.5 and 0.9 for each parameter, and convergences could be obtained. Figs.6—8 show the convergence curves of the 11 parameters. The inverse results are exactly the same as those in Fig.4, which confirms that the Levenberg-Marquardt algorithm is not only accurate but also exhibits convergence stability when used to solve the inverse coupled heat transfer issue.

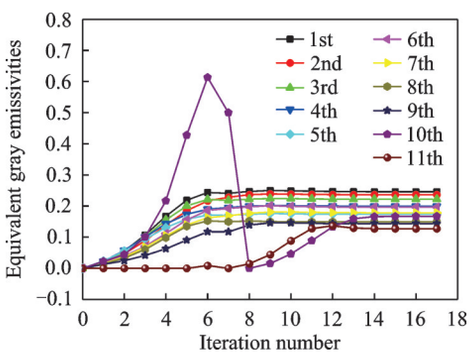

Fig.6 Convergence curves of 11 equivalent gray emissivities with initial guesses as 0.000 01

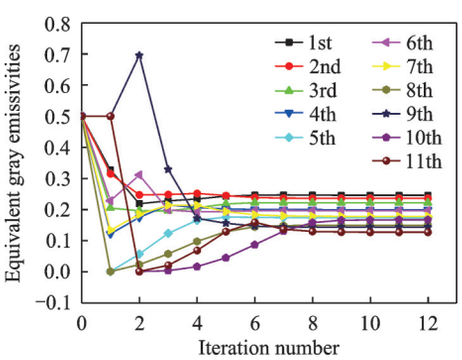

Fig.7 Convergence curves of 11 equivalent gray emissivities with initial guesses as 0.5

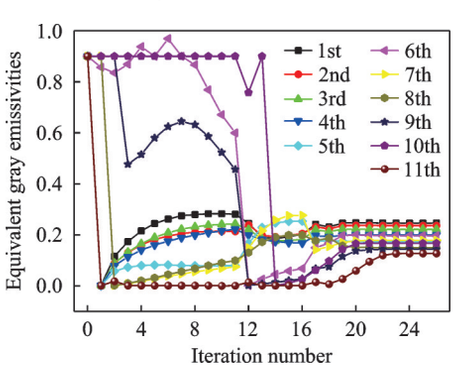

Fig.8 Convergence curves of 11 equivalent gray emissivities with initial guesses as 0.9

It should be emphasized that a modification is implemented in Eq.(13) for determining the damping factor, because the inverse problem is highly nonlinear. The power n in Eq.(13) is not a constant, and it is adjusted in the present work. In order to ensure good convergence stability, n is assumed to be a small value between 0.000 01 and 1.0 if the dimensionless objective function exceeds a given value, such as 10^{-3}. Otherwise, n is a greater value between 2 and 100 to guarantee a high efficiency.

For comparison, effects of initial guesses on inverse results by using the least-squares method are also investigated. The results show that a convergence could be obtained when initial guesses are 0.000 01 or 0.5, and the results are the same as those in Fig.4. However, a convergence could not be obtained when initial guesses are 0.9. The algorithm reliably converges to the optimal solution, providing accurate results for the inverse problem at hand compared to the least-squares method. It is mainly attributed to the introduction of the damping factor in the Levenberg-Marquardt algorithm.

Furthermore, it can be determined that the total number of iterations required for convergence is 17, 12, and 26 for the three cases from Fig.6, Fig.7, and Fig.8, respectively, which also manifests that for the inverse coupled heat transfer problem, the Levenberg-Marquardt algorithm is substantially more effective than the least-squares method.

Another aspect should be emphasized here. The present inverse problem is highly nonlinear, because it is an inverse coupled conduction, convection and radiation problem involving absorbing, emitting, and non-gray participating media. For this kind of problem, the least-squares method could be also efficient, if initial guesses are very close to exact values. However, one could usually give rough initial guesses as in this study. Therefore, the least-squares method is either slow or unstable for solving the present inverse problem.

3.3 Effects of measurement errors

In the inverse analysis illustrated above, the temperature measurements are assumed to be error-free. However, temperature measurements inevitably contain errors when used in actual applications. Two tests are conducted to determine how these inaccuracies affect the inverted findings.

The scenarios described in the Ref. [11] are simulated. In the first test, an overall test data measurement errors of 0.5%, 1.0%, and 1.5% are set. Other calculation conditions are kept the same as those in the above analysis.

Table 3 shows the recovered equivalent gray emissivities, in which ζ represents measurement error. An observation can be made that as ζ rises from 0.5% to 1.5%, the precision of the inverse problem findings decreases. The inverse results progressively deviate further from the exact values as the measurement error grows.

Table 3 Recovered equivalent gray emissivities with different measurement errors

No.	E_{rel}			
	ζ=0%	ζ=0.5%	ζ=1%	ζ=1.5%
1	0.246 13	0.275 29	0.309 16	0.349 15
2	0.236 27	0.256 19	0.278 44	0.303 30
3	0.221 74	0.239 68	0.259 59	0.282 03
4	0.199 63	0.212 09	0.225 63	0.240 12
5	0.173 67	0.186 66	0.201 14	0.217 83
6	0.196 30	0.215 09	0.236 69	0.260 68
7	0.178 37	0.193 45	0.210 37	0.231 83
8	0.149 59	0.159 53	0.170 30	0.182 14
9	0.143 24	0.153 31	0.163 94	0.175 83
10	0.166 96	0.231 13	0.426 86	0.528 75
11	0.127 06	0.182 75	0.211 78	0.223 13

The relative discrepancy E_{rel} is defined as

$$E_{rel}=\left|\frac{\varepsilon-\varepsilon_{exact}}{\varepsilon_{exact}}\right|\times 100\% \tag{15}$$

The inverse heat transfer problem is highly nonlinear due to the presence of radiative transfer and absorption, emission and non-gray radiation properties, so the values of E_{rel} are very great and their values at different measurement errors are given in Table 4. Moreover, all measurements are supposed to contain the same measurement error. However, measurement errors at some measurement points may be very small or could be neglected in practical applications, so the inverse accuracy would be higher in practical applications.

Table 4 Relative errors of recovered equivalent gray emissivities with different measurement errors

No.	E_{rel}		
	ζ=0.5%	ζ=1%	ζ=1.5%
1	11.847 4	25.608 4	41.855 9
2	8.431 0	17.848 2	28.370 1
3	8.090 6	17.069 5	27.189 5
4	6.241 5	13.024 1	20.282 5
5	7.479 7	15.817 4	25.427 5
6	9.572 1	20.575 6	32.796 7
7	8.454 3	17.940 2	29.971 4
8	6.644 8	13.844 5	21.759 5
9	7.030 2	14.451 3	22.752 0
10	38.434 4	155.666 0	216.692 6
11	43.829 7	66.677 2	75.610 0

In the second test, random measurement errors are considered to simulate real practical applications, and their effects on recovered equivalent gray emissivities are investigated. A random error component is incorporated into the precise temperature in order to consider the random measurement error

$$t=t_{exact}\times(1+\zeta\eta/2.576) \tag{16}$$

where η can take on any value within the range of -1 to 1 with equal probability.

Fig.9 shows random numbers imposed on measurements for each measurement error, 0.5%, 1.0% and 1.5%. Convergence could be obtained for each measurement error by using the Levenberg-Marquardt algorithm, and Fig.10 shows the recovered equivalent gray emissivities. As anticipated, the inverse accuracy diminishes as the measurement error increases. For comparison, we also employ the least-squares method to recover the equivalent gray emissivities. A convergence could be achieved if the measurement error is 0.5%, and the results are the same as those by using the Levenberg-Marquardt algorithm. However, convergence could not be obtained even very small relaxation factors are adopted, if the measurement error is 1% or 1.5%. This implies that the Levenberg-Marquardt algorithm performs better in solving the pathological problems of inverse coupled conduction, convection and radiation issue involving absorption, emission, and non-gray participating media. Consequently, it

can be concluded that the Levenberg-Marquardt algorithm demonstrates greater robustness compared to the least-squares method when addressing the current inverse problem. In addition, the Levenberg-Marquardt algorithm with improved convergence stability in solving the current highly nonlinear inverse problem is also verified.

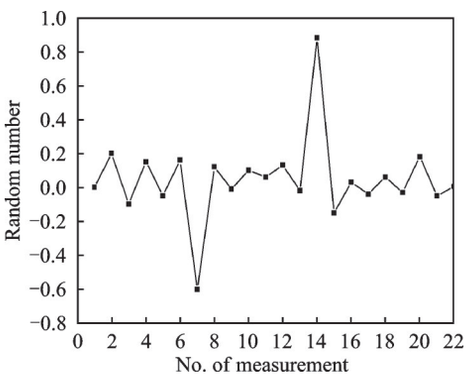

Fig.9 Random numbers imposed on measurements

Fig.10 shows that equivalent gray emissivities could be accurately recovered at low temperatures (with a relatively small number of retrieval parameters), even with measurement errors. However, the results deviate the exact values much at high temperatures. It is because the nonlinear effect, mainly caused by radiation, is heavier at high temperatures for the present inverse coupled heat exchange issue. Therefore, the measurements should be as accurate as possible for accurately solving the inverse problem in real practical applications.

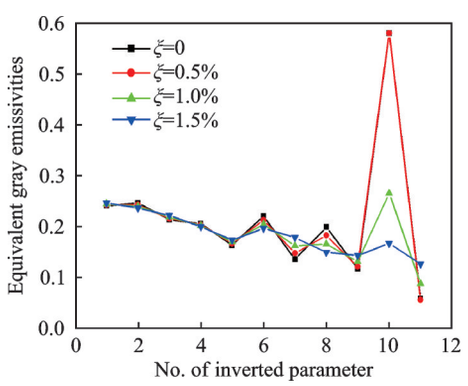

Fig.10 Recovered equivalent gray emissivities with random measurement errors

4 Conclusions

This paper proposes the Levenberg-Marquardt algorithm to address an inverse coupled heat transfer issue in a reheating furnace incorporating absorption, emission, and non-gray participating media. The algorithm is shown to effectively recover comparable gray radiative characteristics of non-gray media. In order to enhance the efficacy of this algorithm's performances, a modification has been incorporated into the recently proposed formulation for determining the damping factor. It is comprehensively investigated whether high accuracy, great efficiency, convergence stability and good robustness can be guaranteed when this algorithm solves the inverse problem.

The results show that the Levenberg-Marquardt algorithm is with high accuracy for recovering the comparable gray radiative properties. The issue of low inverse efficiency in solving the current inverse problem can be effectively addressed, which means that the Levenberg-Marquardt algorithm is more efficient than the least-squares method. Moreover, in the context of highly nonlinear inverse problems, the Levenberg-Marquardt algorithm demonstrates superior convergence stability and robustness. It is mainly attributed to the introduction of the damping factor in the Levenberg-Marquardt algorithm. In addition, the newly presented formulation for determining the damping factor and its modification in the present work could guarantee both high efficiency and good convergence stability.

References

[1] SIMONETTI M, CAILLOL C, HIGELIN P, et al. Experimental investigation and 1D analytical approach on convective heat transfers in engine exhaust-type turbulent pulsating flows[J]. Applied Thermal Engineering, 2020, 165: 114548.

[2] XU J X, LI B K, QI F S, et al. Modeling effects of skid buttons and dislocated skids on the heating quality of slabs in an industrial walking-beam reheating furnace[J]. International Journal of Heat and Mass Transfer, 2023, 211: 124245.

[3] HAN W C, REN R D. Simulation of aircraft electrothermal windshield heat transfer with artificial heat source method[J]. Transactions of Nanjing University of Aeronautics and Astronautics, 2023, 40(S1): 50-54.

[4] BAHRAMI A, SAFAVINEJAD A, AMIRI H. Analysis of spectral radiative entropy generation in a non-gray planar participating medium at radiative equilibrium with two different boundary conditions[J]. International Journal of Thermal Sciences, 2019, 146:

106073.

[5] BORDBAR H, HYPPÄNEN T. Line by line based band identification for non-gray gas modeling with a banded approach[J]. International Journal of Heat and Mass Transfer, 2018, 127: 870-884.

[6] YANG Y, ZHENG S, LU Q. Numerical solutions of non-gray gases and particles radiative transfer in three-dimensional combustion system using DRESOR and SNBCK[J]. International Journal of Thermal Sciences, 2021, 161: 106783.

[7] LIU H D, ZHOU H C, HONG W P, et al. Key parameter analysis of the DRESOR method for calculating the radiative heat transfer in three-dimensional absorbing, emitting and scattering media[J]. International Journal of Thermal Sciences, 2021, 168: 107047.

[8] SUN Y J, ZHANG X B. Contributions of gray gases in SLW for non-gray radiation heat transfer and corresponding accuracies of FVM and P1 method[J]. International Journal of Heat and Mass Transfer, 2018, 121: 819-831.

[9] SUN Y J, ZHANG X B, HOWELL J R. Non-gray combined conduction and radiation heat transfer by using FVM and SLW[J]. Journal of Quantitative Spectroscopy and Radiative Transfer, 2017, 197: 51-59.

[10] LUO X C, YANG Z. A new approach for estimation of total heat exchange factor in reheating furnace by solving an inverse heat conduction problem[J]. International Journal of Heat and Mass Transfer, 2017, 112: 1062-1071.

[11] CUI M, GAO X W, CHEN H G. A new inverse approach for the equivalent gray radiative property of a non-gray medium using a modified zonal method and the complex-variable-differentiation method[J]. Journal of Quantitative Spectroscopy and Radiative Transfer, 2011, 112(8): 1336-1342.

[12] BANGIAN-TABRIZI A, JALURIA Y. A study of transient wall plume and its application in the solution of inverse problems[J]. Numerical Heat Transfer, Part A: Applications, 2019, 75(3): 149-166.

[13] ZHOU L, ZHANG C Y, BAI Y S, et al. Improved particle swarm optimization for solving transient nonlinear inverse heat conduction problem in complex structure[J]. Transactions of Nanjing University of Aeronautics and Astronautics, 2021, 38(5): 816-828.

[14] MOSAVATI B, MOSAVATI M. A new approach to solve inverse boundary design of a radiative enclosure with specular-diffuse surfaces[J]. Journal of Heat Transfer, 2022, 144(1): 012801.

[15] OMARAA E, FARAH S, ALEMU A, et al. Mathematical modelling of heat transmission in the temperature history apparatus by using inverse method to evaluate the latent heat of high temperature PCMs[J]. International Journal of Heat and Mass Transfer, 2021, 167: 120825.

[16] ZHAO T, SUN Q H, XIN Y L, et al. A generalized Benders decomposition-based algorithm for heat conduction optimization and inverse design[J]. International Journal of Heat and Mass Transfer, 2023, 211: 124224.

[17] ZHANG C Y, HE Z, LV J, et al. Inverse estimation of effective thermal conductivity of multilayer materials considering thermal contact resistance[J]. ASME Journal of Heat and Mass Transfer, 2023, 145(8): 084501.

[18] LEE K H. Application of repulsive particle swarm optimization for inverse heat conduction problem-parameter estimations of unknown plane heat source[J]. International Journal of Heat and Mass Transfer, 2019, 137: 268-279.

[19] FAN X H, ZHANG Z Y, ZHU J, et al. Systematic investigations on doping dependent thermal transport properties of single crystal silicon by time-domain thermoreflectance measurements[J]. International Journal of Thermal Sciences, 2022, 177: 107558.

[20] GE W J, DAVID C, MODEST M F, et al. Comparison of spherical harmonics method and discrete ordinates method for radiative transfer in a turbulent jet flame[J]. Journal of Quantitative Spectroscopy and Radiative Transfer, 2023, 296: 108459.

[21] XIONG P, DENG J, LU T, et al. A sequential conjugate gradient method to estimate heat flux for nonlinear inverse heat conduction problem[J]. Annals of Nuclear Energy, 2020, 149: 107798.

[22] JOACHIMIAK M, JOACHIMIAK D, CIAŁKOWSKI M, et al. Analysis of the heat transfer for processes of the cylinder heating in the heat-treating furnace on the basis of solving the inverse problem[J]. International Journal of Thermal Sciences, 2019, 145: 105985.

[23] WANG Y J, SUN W J, GAO Q H, et al. Numerical study on flow and heat transfer characteristics inside rotating rib-roughened pipe with axial throughflow[J]. Transactions of Nanjing University of Aeronautics and Astronautics, 2023, 40(5): 522-533.

[24] BAI Y S, ZHANG C Y, HE Z, et al. Inverse solution to two-dimensional transient coupled radiation and conduction problems and the application in recovering radiative thermo-physical properties of Si_3N_4 ceramics[J]. International Journal of Thermal Sciences, 2023, 190: 108303.

[25] SINGHAL M, SINGH S, SINGLA R K, et al. Experimental and computational inverse thermal analysis of transient, non-linear heat flux in circular pin fin with temperature-dependent thermal properties[J]. Applied Thermal Engineering, 2020, 168: 114721.
[26] LYNESS J N, MOLER C B. Numerical differentiation of analytic functions[J]. SIAM Journal on Numerical Analysis, 1967, 4(2): 202-210.
[27] CUI M, ZHAO Y, XU B B, et al. A new approach for determining damping factors in Levenberg-Marquardt algorithm for solving an inverse heat conduction problem[J]. International Journal of Heat and Mass Transfer, 2017, 107: 747-754.
[28] JI W C, LI G J, WEI L Y, et al. An improved sequential quadratic programming method for identifying the total heat exchange factor of reheating furnace[J]. International Journal of Thermal Sciences, 2024, 204: 109238.
[29] YI Z, SU Z G, LI G J, et al. Development of a double model slab tracking control system for the continuous reheating furnace[J]. International Journal of Heat and Mass Transfer, 2017, 113: 861-874.
[30] SKOPEC P, VYHLÍDAL T, KNOBLOCH J. Development of a continuous reheating furnace state-space model based on the finite volume method[J]. Applied Thermal Engineering, 2024, 246: 122888.
[31] CUI M, GAO X W, CHEN H G. Inverse radiation analysis in an absorbing, emitting and non-gray participating medium[J]. International Journal of Thermal Sciences, 2011, 50(6): 898-905.
[32] CUI M. Dynamical compensation of total heat exchange factor based on non-gray radiation properties of gas in reheating furnace[D]. Liaoning, China: Northeastern University, 2009. (in Chinese)

Acknowledgements This work was supported by the National Natural Science Foundation of China (No.12172078); and the Fundamental Research Funds for the Central Universities (No. DUT24MS007).

Authors Mr. **HE Zheng** is currently pursuing his M.S. degree in School of Mechanics and Aerospace Engineering, Dalian University of Technology. He obtained his Bachelor's degree in 2022. His research focuses on prediction methods for equivalent radiative properties of non-gray participating media.

Prof. **CUI Miao** recieved her Ph.D. degree from Northeastern University in 2009. She is currently a professor and doctoral supervisor in School of Mechanics and Aerospace Engineering, Dalian University of Technology, in response to the major needs of thermal protection system for hypersonic vehicles. She has devoted to the research of new numerical methods for multi-field coupling and inverse problem solving.

Author contributions Mr. **HE Zheng** interpreted the results and wrote the manuscript. Mr. **CAO Zhenkun** contributed to the discussion and background of the study. Mr. **CHENG Xiang** contributed to data analysis. Prof. **CUI Miao** designed the study and reviewed the manuscript. Mr. **LIU Kun** made the data curation. All authors commented on the manuscript draft and approved the submission.

Competing interests The authors declare no competing interests.

(Production Editor: ZHANG Bei)

求解非灰介质参与的导热-对流-辐射耦合传热问题的快速逆分析

何 峥[1], 曹振坤[1], 程 响[2], 崔 苗[1], 刘 焜[1]

(1.大连理工大学力学与航空航天学院, 工业装备结构分析优化与CAE软件全国重点实验室, 大连 116024, 中国; 2.中国运载火箭技术研究院空间物理重点实验室, 北京 100076, 中国)

摘要:吸收、发射和非灰体参与的加热炉介质中的非灰辐射特性的存在,使得求解辐射传热问题变得复杂,并进一步增加了导热-对流-辐射耦合传热问题的求解难度,导致效率低下,且无法满足实时控制需求。为了克服这些困难,本文提出通过求解反问题预测非灰介质的等效灰体辐射特性。然而,采用最小二乘法所需的迭代次数很多,导致反演效率很低,因此亟需一种高效快速的方法。本文采用列文伯格-马夸尔特(Levenberg-Marquardt)算法求解耦合传热反问题,预测了等效灰体辐射特性,旨在解决采用最小二乘法时的反演效率低的问题。为提升列文伯格-马夸尔特算法的性能,本文对阻尼因子的确定方法进行了改进,并且对该算法的准确性、收敛稳定性、效率和鲁棒性进行了详细研究。最后,对两种方法获得的结果进行了比较。

关键词:反问题;耦合传热问题;列文伯格-马夸尔特算法